Original Article

Low expression of *KLRB1* predicts poor survival outcomes and is associated with immune infiltration in breast cancer

Xiao Liu[1], Qianqian Cui[1,2], Nan Qin[1]

[1]Department of Breast Surgery, Cancer Hospital of China Medical University, Liaoning Cancer Hospital & Institute, Shenyang, China; [2]Department of Breast Surgery, Altaira Nursing Service, Campbelltown, SA, Australia

Contributions: (I) Conception and design: Q Cui, X Liu; (II) Administrative support: N Qin; (III) Provision of study materials or patients: X Liu; (IV) Collection and assembly of data: X Liu; (V) Data analysis and interpretation: Q Cui; (VI) Manuscript writing: X Liu; (VII) Final approval of manuscript: All authors.

Correspondence to: Nan Qin, MN. Department of Breast Surgery, Cancer Hospital of China Medical University, Liaoning Cancer Hospital & Institute, No. 44 Xiaohuayuan Road, Dadong District, Shenyang 110042, China. Email: qn84623@163.com.

Background: *KLRB1* is downregulated in various cancer types. Nevertheless, the specific involvement of *KLRB1* in the context of breast cancer (BRCA) has not been fully elucidated. This research aimed to explore its clinical value in BRCA.

Methods: A dataset comprising 1,109 BRCA samples and 113 healthy samples was retrieved from The Cancer Genome Atlas (TCGA) database to establish the association between *KLRB1* expression and pan-cancer. Subsequently, an analysis was executed to explore the link between *KLRB1* and BRCA. T-tests and Chi-squared tests were conducted to assess the expression of *KLRB1* and its clinical implications in BRCA. The prognosis-predictive value of *KLRB1* in BRCA was assessed using the Kaplan–Meier method and Cox regression analysis. Gene Ontology (GO) and Kyoto Encyclopedia of Genes and Genomes (KEGG) enrichment analyses screened biological pathways to analyze the association between the immune infiltration level and *KLRB1* expression in BRCA. Lastly, the conclusion was validated through quantitative polymerase chain reaction (qPCR), immunohistochemistry (IHC), and Cell Counting Kit-8 (CCK8) assays.

Results: *KLRB1* exhibited low expression in patients with BRCA. Furthermore, *KLRB1* demonstrated strong diagnostic potential, as indicated by an area under curve (AUC) of 0.712. Kaplan-Meier survival and Cox regression analyses indicated that attenuated expression of *KLRB1* was independently linked to unfavorable clinical outcomes. GO and KEGG enrichment analyses were performed on the top 10 genes that exhibited positive and negative correlations with *KLRB1*. Analysis of genes positively correlated with *KLRB1* revealed associations with signaling receptor activator activity, lymphocyte proliferation, mononuclear cell proliferation, leukocyte proliferation, receptor-ligand activity, immunoglobulin binding, and hematopoietic cell lineage signaling pathway. *KLRB1* expression exhibited significant correlations with all immune cells. Furthermore, qPCR and IHC outcomes demonstrated that *KLRB1* was significantly downregulated in BRCA tissues. CCK8 findings showed a decrease in the proliferation of BRCA MCF7 cells upon knockout of *KLRB1*.

Conclusions: This research investigated the mechanism and potential therapeutic target of the *KLRB1* gene in BRCA. By analyzing the expression and function of the *KLRB1* gene, the study aims to find its significant role in the onset and progression of BRCA. This research endeavors to offer novel strategies and approaches for treating BRCA.

Keywords: *KLRB1*; immune; breast cancer (BRCA); prognosis

Submitted Jul 14, 2023. Accepted for publication Feb 08, 2024. Published online Mar 25, 2024.
doi: 10.21037/tcr-23-1231
View this article at: https://dx.doi.org/10.21037/tcr-23-1231

Introduction

Globally, the burden of breast cancer (BRCA) is increasing. This disease stands as the most prevalent type of cancer in females and a leading contributor to cancer-related mortality (1,2). While advancements in early diagnosis and comprehensive treatment approaches have led to improved prognoses for individuals with BRCA, the 5-year overall survival (OS) rate remains below 20% when metastasis is present (3,4). Hence, there is an urgent need to identify biological markers associated with BRCA prognosis.

Recent research has indicated a potential close association between the *KLRB1* gene and the onset and progression of BRCA (5). *KLRB1* gene is a cell surface molecule belonging to the C-type lectin family and has a variety of biological functions (6). In the immune response, the *KLRB1* gene can inhibit the activation of T lymphocytes, thus playing an immunomodulatory role (7). Multiple investigations have explored the expression and role of the *KLRB1* gene in BRCA. These studies have frequently revealed a reduced expression or deletion of the *KLRB1* gene within BRCA cells, showcasing a strong association with the invasive and metastatic tendencies of tumors (8,9). Additionally, the *KLRB1* gene can affect the biological behavior of BRCA cells by regulating cell apoptosis, cell cycle, cell invasion, and other processes (10). In addition, recent research also found that the *KLRB1* gene may be associated with chemotherapy resistance of BRCA, offering a novel potential target for BRCA treatment (11). However, the role of the *KLRB1* gene in BRCA remains uncertain. Therefore, this study aims to explore the mechanism and potential therapeutic targets of the *KLRB1* gene in BRCA.

As high-throughput sequencing technology has advanced, the generation of extensive omics data has become feasible (12,13,14). The The Cancer Genome Atlas (TCGA)-BRCA gene can help elucidate the causes and prognosis of cancer. This research analyzed the transcriptional levels and prognosis-predictive value of *KLRB1* using the data acquired from TCGA-BRCA. Furthermore, the biological mechanism of *KLRB1* was investigated using Gene Ontology (GO) and Kyoto Encyclopedia of Genes and Genomes (KEGG) analyses, and the relationship between *KLRB1* and immune infiltration levels was assessed. Additionally, quantitative polymerase chain reaction (qPCR), immunohistochemistry (IHC), and Cell Counting Kit-8 (CCK8) experiments provided validation for our findings. We present this article in accordance with the TRIPOD reporting checklist (available at https://tcr.amegroups.com/article/view/10.21037/tcr-23-1231/rc).

Highlight box

Key findings

- KLRB1 is a potential predictive tumor marker for breast cancer (BRCA) patients.

What is known and what is new?

- BRCA seriously endangers women's health. It is the most commonly diagnosed cancer in women, and ranks second among the causes of cancer-related deaths in women.
- The high expression of KLRB1 is associated with prognostic significance.

What is the implication, and what should change now?

- By analyzing the expression and function of KLRB1 gene, we expect to find its important role in the occurrence and development of BRCA, and provide new strategies and methods for the treatment of BRCA.
- Report about implications and actions is needed.

Methods

Data processing

Expression profiles of 1,109 BRCA tissues and 113 adjoining tissues were retrieved from TCGA. Subsequently, clinicopathological features and predictive data of the individuals were subjected to further screening. RNA-seq (RNA sequencing) data in transcripts per kilobase million (TPM) format from TCGA were uniformly processed. The expression of *KLRB1* was evaluated using TCGA. To assess the level of *KLRB1* expression in the pan-cancer, extracted data from UCSC Xena were assessed (https://xenabrowser.net/datapages/).

Patients and tissues

Ten pairs of BRCA samples and their matched non-tumor tissues were acquired from Liaoning Cancer Hospital. Every participant provided written informed consent. The approval for this research was granted by the ethics committee of Liaoning Cancer Hospital (20210621) and the study was conducted in accordance with the Declaration of Helsinki (as revised in 2013). The BRCA tissues were collected post-surgery, immediately frozen in liquid nitrogen, and then preserved at –80 ℃ for qPCR analysis.

Gene enrichment analysis

By utilizing the transcriptional sequence from TCGA, the

study employed GO and KEGG analyses to determine the genes and pathways associated with *KLRB1*. The expression data were classified into groups with high and low *KLRB1* expression (R "clusterProfiler").

Immune cell infiltration

To evaluate the relative abundance of infiltrating immune cells in tumor tissues, single sample gene set enrichment analysis (ssGSEA) was conducted. The infiltration levels of immune cells in BRCA expression data were assessed utilizing R "gsva" and an immune data set, including 24 immune cells.

Survival and prognosis analysis

The "survival" graph of *KLRB1* was utilized to derive the OS. A division threshold of 50% was chosen as a critical value to divide the cohort into high- and low-expression groups. To examine the prognostic significance of *KLRB1* in individuals with BRCA, the "roc" function from the R package was employed for analysis, and visualization was performed using the "ggplot2" package.

Cell culture and transfection

The MCF10A cell line, MCF7 cell line and MDAMB231 cell line was acquired from the Chinese Academy of Sciences and cultured in minimum essential medium (MEM) comprising 10% fetal bovine serum (FBS; GIBCO, Waltham, MA, USA) and 1% penicillin-streptomycin. Cells were cultured in a humidified incubator under 5% CO_2 at 37 ℃. One day prior to transfection, MCF7 and MDAMB231 cells were cultured in six-well plates to achieve 50–60% confluence. Transfection of the *KLRB1*-targeted pEZ-M03 vector was carried out using Lipofectamine 2000 (Thermo Fisher Scientific, Waltham, MA, USA) as per the provided guidelines.

RNA isolation and qPCR analysis

The extraction of tissue RNA was carried out using the TRIzol reagent (Invitrogen, Carlsbad, CA, USA). Subsequently, the extracted RNA was converted into complementary DNA (cDNA) using the QuantiTect Reverse Transcription Kit (Qiagen, Valencia, CA, USA). The qPCR technique quantifies DNA during each cycle of the PCR reaction through real-time fluorescence measurements. The analyses were conducted using SYBR-Green (Takara, Otsu, Shiga, Japan) as the detection dye, with GAPDH serving as the internal control. The primers employed were as follows: KLRB1 forward primer, 5'-AATTTGCCCTGAAACTTAGCTG-3'; reverse, 5'-GGATGTCACTGAAACACTCAAC-3'. GAPDH forward primer, 5'-GTCTCCTCTGACTTCAACAGCG-3'; reverse, 5'-ACCACCCTGTTGCTGTAGCCAA-3'. The qPCR value was calculated using the 2-delta delta Ct method. We set the Ct value to 15-35, and Ct values not in this range will be excluded.

IHC

IHC was performed using a two-step method according to the manufacturer's instructions (PV-9000; ZSGB-BIO, Beijing, China). BRCA samples were fixed in 10% formalin, paraffin-embedded, and sectioned into 5-μm slices. The samples were de-waxed with ethanol and blocked to inactivate the endogenous peroxidase activity. Subsequently, antigen retrieval was achieved by heating the samples in a microwave, followed by cooling to room temperature. Blocking was performed using goat serum for 30 minutes at 37 ℃. The samples were then incubated overnight at 4 ℃ with rabbit anti-KLRB1 (Thermo Fisher Scientific 17-5941-82) (1:200). Afterward, incubation with horseradish peroxidase-coupled goat anti-rabbit secondary antibody (PV-9000; ZSGB-BIO, Beijing, China) was conducted at 37 ℃ for 30 minutes. The samples were then stained with 3,3'-diaminobenzidine (DAB). Cell nuclei were stained blue with hematoxylin. The sections were then dehydrated, cleared with xylene, and mounted. KLRB1 expressions were determined by IHC using the streptavidin peroxidase method, with adjacent tissues serving as the controls. The experimental procedure was performed as per the manufacturer's instructions. Image-Pro Plus 6.0 Software (Media Cybernetics, USA) was used to analyze protein expression and perform statistical analysis of the results obtained by IHC.

Cell colony formation assay

The cells were planted at a density of 1×10^3/mL in each well of the 6-well plates, with 2 mL of MEM medium supplemented with 10% FBS, 100 U/mL penicillin, and 100 μg/mL streptomycin. Single-cell-derived clones were allowed to grow for ten days. Prior to fixation, the culture was pre-cooled three times with phosphate buffered

saline (PBS). The cells were then fixed with methanol for 15 minutes, stained with crystal violet for 20 minutes, and rinsed with water. The dishes were air dried, and the number of visible clones was visually counted. The colony formation rate was calculated. This entire procedure was repeated three times to ensure reproducibility.

Transwell assay

The cells were collected, resuspended in serum-free media, and introduced into the upper compartment of a Transwell membrane filter that had been coated with Matrigel (Corning) for invasion assays. To the lower compartment, we added a culture medium containing 10% FBS and either 0, 5, or 10 nM Tanespimycin as a chemoattractant. After a 36-hour incubation period, the cells were fixed with methanol, stained with 0.1% crystal violet, and then imaged and counted using an Olympus microscope (Tokyo, Japan). For the migration assay, the process was repeated for 24 hours.

Statistical analysis

The Wilcoxon rank-sum test was employed to conduct statistical analysis on the expression of *KLRB1* in both the healthy and BRCA groups. Individuals were classified into two groups as per their "median" expression of *KLRB1*. The clinical and pathological characteristics of *KLRB1* were assessed utilizing the Wilcoxon-rank sum test or Kruskal-Wallis test and logistic regression. Prognosis-predictive analysis was conducted utilizing Kaplan-Meier analysis as well as univariate and multivariate Cox analyses. The diagnostic value of differentially expressed genes (DEGs) was analyzed by generating a receiver operating characteristic (ROC) curve utilizing the "proc" package.

Results

Expression analysis of KLRB1 in pan-cancer and BRCA

Data downloaded from TCGA and Genotype-Tissue Expression (GTEX) were used to evaluate the expression of *KLRB1* in 33 cancers. The results demonstrated that *KLRB1* exhibited low expression in various cancer types, including BRCA, bladder urothelial carcinoma (BLCA), kidney chromophobe (KICH), colon adenocarcinoma (COAD), pancreatic adenocarcinoma (PAAD), liver hepatocellular carcinoma (LIHC), head and neck squamous cell carcinoma (HNSC), lung adenocarcinoma (LUAD), rectum adenocarcinoma (READ), lung squamous cell carcinoma (LUSC), thyroid carcinoma (THCA) and uterine corpus endometrial carcinoma (UCEC). However, the expression of *KLRB1* was high in kidney renal clear cell carcinoma (KIRC), glioblastoma multiforme (GBM), and kidney renal papillary cell carcinoma (KIRP) (*Figure 1A*). The link between *KLRB1* expression and clinical outcomes of individuals with BRCA was further investigated. Survival analysis demonstrated remarkable variations among distinct cancer types (*Figure 1B-1D*). Within the BRCA cohort, individuals exhibiting elevated *KLRB1* levels displayed extended OS, progression-free interval (PFI), and disease-specific survival (DSS) in contrast to those with lowered *KLRB1* levels. Furthermore, the evaluation of *KLRB1* expression in BRCA within the TCGA database provided confirmation of its lower expression in this context (*Figure 1E,1F*). *KLRB1* messenger RNA (mRNA) expression in human epidermal growth factor receptor 2 (HER2), Luminal A, Luminal B and triple negative breast cancer (TNBC) tissues were no significant difference (*Figure 1G*). And gene deletion was an important factor for *KLRB1* down-regulation in BRCA (*Figure 1H*).

Clinical correlation of KLRB1 expression in individuals with BRCA

The clinical features and gene expression profiles of 1083 individuals with primary BRCA were acquired from the TCGA database. Individuals were classified into high (n=542) and low (n=541) *KLRB1* expression groups. The aim was to examine the link between the *KLRB1* expression and the clinical and pathological attributes of individuals. The analysis demonstrated a link between *KLRB1* expression and M stage (P=0.043) as well as age (P<0.001), utilizing the chi-square test or Fisher's exact test (*Table 1*).

Link between KLRB1 expression and survival prognosis of individuals with BRCA

Univariate and multivariate Cox analyses were conducted to examine the impact of various factors on the OS of BRCA patients, as detailed in *Table 2*. In the univariate Cox analysis, *KLRB1* expression (P<0.001), T3&T4 stage (P=0.006), N stage (P<0.001), M1 stage (P<0.001), pathological stage III&IV (P<0.001), and age >60 (P<0.001) were linked to the OS. The multivariate Cox model revealed an association with poor prognosis for age >60

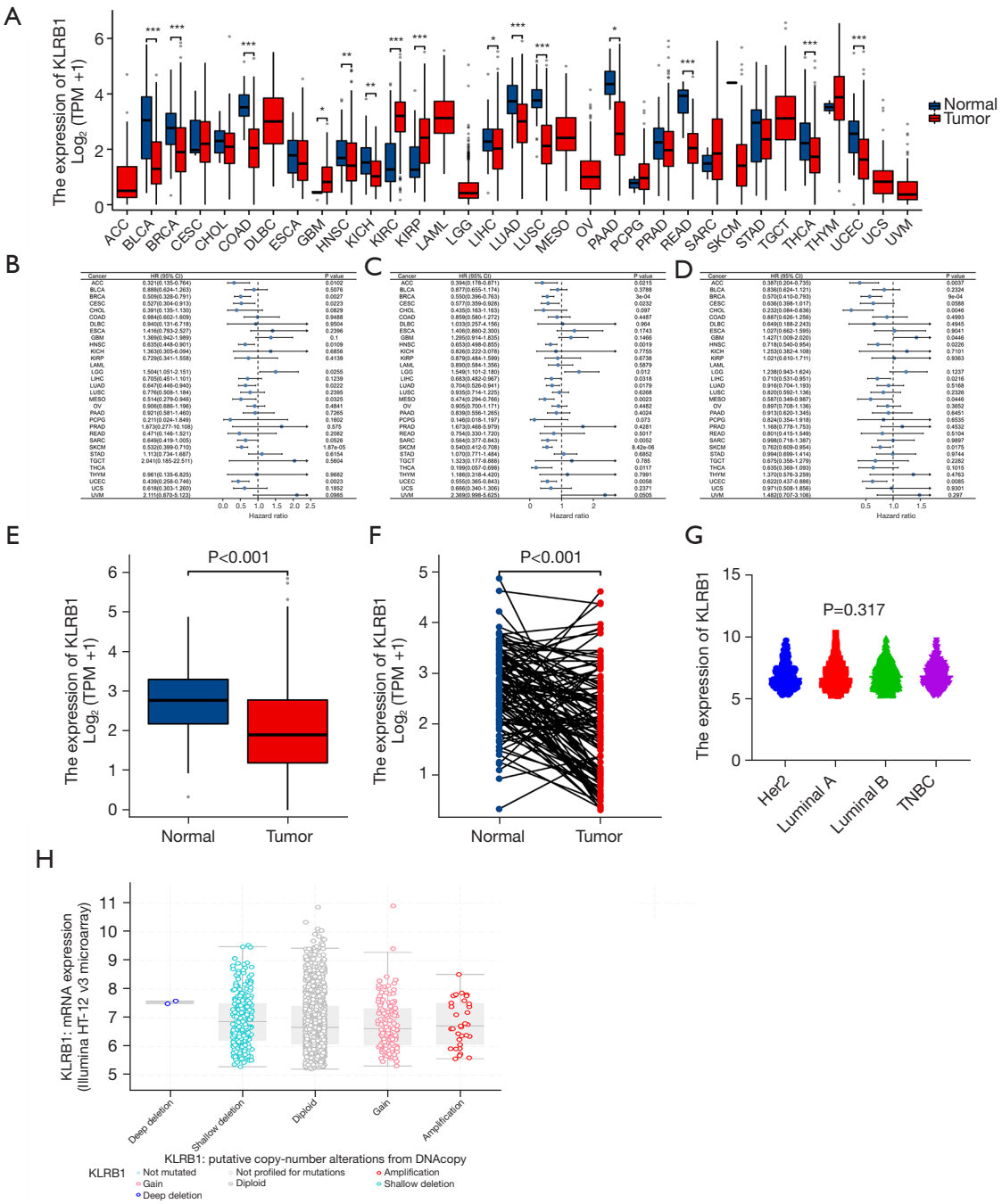

Figure 1 Association between *KLRB1* mRNA expression level and prognosis based on TCGA database. (A) The mRNA expression of *KLRB1* in distinct cancer tissues and adjoining healthy tissues. (B) Prognostic correlation between *KLRB1* expression and distinct cancer types (OS). (C) Prognostic correlation between *KLRB1* expression and distinct cancer types (DSS). (D) Prognostic association between *KLRB1* expression and various cancer types (PFI). (E) *KLRB1* mRNA expression in BRCA tissues and healthy tissues. (F) *KLRB1* mRNA expression in BRCA tissues and paired sample tissues [right represents HR >1 (risky); left represents HR <1 (protective)]. (G) *KLRB1* mRNA expression in HER2, luminal A, luminal B and TNBC tissues. (H) Putative copy-number alterations of *KLRB1* in BRCA. *, P<0.05; **, P<0.01; ***, P<0.001. mRNA, messenger RNA; TCGA, The Cancer Genome Atlas; OS, overall survival; PFI, progression-free interval; DSS, disease-specific survival; BRCA, breast cancer; HR, hazard ratio; CI, confidence interval; TPM, transcripts per kilobase million; HER2, human epidermal growth factor receptor 2; TNBC, triple negative breast cancer.

Table 1 *KLRB1* expression in BRCA patients with different clinical parameters

Characteristics	Low expression of *KLRB1* (n=541)	High expression of *KLRB1* (n=542)	P
T stage, n (%)			0.371
T1	132 (12.2)	145 (13.4)	
T2	321 (29.7)	308 (28.5)	
T3	64 (5.9)	75 (6.9)	
T4	21 (1.9)	14 (1.3)	
N stage, n (%)			0.288
N0	268 (25.2)	246 (23.1)	
N1	173 (16.3)	185 (17.4)	
N2	52 (4.9)	64 (6.0)	
N3	33 (3.1)	43 (4.0)	
M stage, n (%)			0.043
M0	447 (48.5)	455 (49.3)	
M1	15 (1.6)	5 (0.5)	
Pathologic stage, n (%)			0.070
Stage I	85 (8.0)	96 (9.1)	
Stage II	321 (30.3)	298 (28.1)	
Stage III	110 (10.4)	132 (12.5)	
Stage IV	13 (1.2)	5 (0.5)	
Race, n (%)			0.204
Asian	34 (3.4)	26 (2.6)	
Black or African American	97 (9.8)	84 (8.5)	
White	361 (36.3)	392 (39.4)	
Age (years), n (%)			<0.001
≤60	267 (24.7)	334 (30.8)	
>60	274 (25.3)	208 (19.2)	
PR status, n (%)			0.436
Negative	163 (15.8)	179 (17.3)	
Indeterminate	1 (0.1)	3 (0.3)	
Positive	346 (33.5)	342 (33.1)	
ER status, n (%)			0.165
Negative	107 (10.3)	133 (12.9)	
Indeterminate	1 (0.1)	1 (0.1)	
Positive	403 (38.9)	390 (37.7)	
HER2 status, n (%)			0.495
Negative	255 (35.1)	303 (41.7)	
Indeterminate	6 (0.8)	6 (0.8)	
Positive	80 (11.0)	77 (10.6)	
Age (years), median [IQR]	61 [51, 70]	55 [47, 64]	<0.001

BRCA, breast cancer; PR, progesterone receptor; ER, estrogen receptor; HER2, human epidermal growth factor receptor 2; IQR, interquartile range.

Table 2 Univariate analysis and multivariate analysis of the correlation between clinicopathological characteristics and OS in BRCA

Characteristics	Total (N)	Univariate analysis		Multivariate analysis	
		Hazard ratio (95% CI)	P value	Hazard ratio (95% CI)	P value
Pathologic T stage	1,083		0.023		
T1	277	Reference		Reference	
T2	631	1.334 (0.889–2.003)	0.164	0.904 (0.372–2.199)	0.824
T3 & T4	175	1.931 (1.208–3.088)	0.006	2.210 (0.740–6.604)	0.156
Pathologic N stage	1,067		<0.001		
N0	516	Reference		Reference	
N1	358	1.947 (1.322–2.865)	<0.001	1.480 (0.686–3.193)	0.317
N2	116	2.522 (1.484–4.287)	<0.001	1.265 (0.349–4.590)	0.720
N3	77	4.191 (2.318–7.580)	<0.001	2.835 (0.794–10.117)	0.108
Pathologic M stage	925		<0.001		
M0	905	Reference		Reference	
M1	20	4.266 (2.474–7.354)	<0.001	1.796 (0.613–5.264)	0.286
Pathologic stage	1,062		<0.001		
Stage I	181	Reference		Reference	
Stage II	619	1.703 (0.989–2.933)	0.055	0.948 (0.289–3.118)	0.931
Stages III & IV	262	3.566 (2.042–6.228)	<0.001	1.980 (0.338–11.606)	0.449
Age (years)	1,086		<0.001		
≤60	603	Reference		Reference	
>60	483	2.024 (1.468–2.790)	<0.001	3.326 (1.972–5.612)	<0.001
PR status	1,033		0.068		
Negative	342	Reference		Reference	
Positive	691	0.729 (0.521–1.019)	0.065	0.972 (0.434–2.176)	0.945
ER status	1,036		0.070		
Negative	240	Reference		Reference	
Positive	796	0.709 (0.493–1.019)	0.063	0.394 (0.167–0.927)	0.033
HER2 status	717		0.074		
Negative	560	Reference		Reference	
Positive	157	1.593 (0.973–2.609)	0.064	1.019 (0.564–1.840)	0.950
KLRB1	1,086		<0.001		
Low	543	Reference		Reference	
High	543	0.550 (0.396–0.763)	<0.001	0.476 (0.290–0.780)	0.003

OS, overall survival; BRCA, breast cancer; CI, confidence interval; PR, progesterone receptor; ER, estrogen receptor; HER2, human epidermalgrowth factor receptor 2.

(P<0.001), estrogen receptor (ER) status positive (P=0.033), and *KLRB1* expression (P=0.003) (*Table 2*). Furthermore, the link between *KLRB1* expression and OS, DSS, and PFI in individuals with BRCA was investigated. The Kaplan-Meier (KM) diagram illustrated that elevated *KLRB1* expression was associated with a poorer prognosis for OS [hazard ratio (HR) 0.55, 95% confidence interval (CI): 0.40–0.76, P<0.001] (*Figure 2A*). Regarding DSS, individuals with elevated *KLRB1* levels still exhibited a poorer prognosis (HR 0.51, 95% CI: 0.33–0.79, P=0.003) (*Figure 2B*). Similarly, for PFI, individuals with elevated *KLRB1* expression also experienced a poorer prognosis (HR 0.57, 95% CI: 0.41–0.79, P<0.001) (*Figure 2C*). However, the low expression of *KLRB1* has no significant difference in the prognosis of BRCA patients with different subtypes (*Figure 2D*). Furthermore, ROC curve analysis was conducted to assess the capability of differentiating BRCA tissues from healthy breast tissues as per *KLRB1* expression levels. The area under the ROC curve (AUC) was 0.712 (*Figure 2E*). Hence, *KLRB1* may become a promising prognostic biological marker for patients with BRCA.

Survival analysis

Subsequently, univariate and multivariate analyses were conducted. In the former, reduced expression of T3 and T4 within the T stage, N1, N2, and N3 within the N stage, M1 within the M stage, stages 3 and 4 within the pathological stage, age >60, and *KLRB1* were linked to OS. The subsequent multivariate analysis indicated independent risk factors. Specifically, age >60, ER status Positive, and reduced expression of *KLRB1* were identified as independent predictive factors for OS among inpatients with BRCA (*Table 2* and *Figure 3*).

Enrichment analysis of KLRB1-related genes

A total of 24,593 genes exhibited differential expression between the groups characterized by low and high *KLRB1* expression levels, including 8 genes with lowered expression levels and 20 genes with elevated expression levels (adjusted P value <0.05, |log2 fold change (FC)|>3) (*Figure 4A* and table available at https://cdn.amegroups.cn/static/public/tcr-23-1231-1.xlsx). The results of GO and KEGG joint analysis of DEGs demonstrated that it was mainly enriched in signaling receptor activator activity, lymphocyte proliferation, mononuclear cell proliferation, leucocyte proliferation, receptor-ligand activity, immunoglobulin binding and hematopoietic cell lineage signaling pathways (*Figure 4B* and *Table 3*). Moreover, the GSEA of the detected DEGs revealed several immune-related biological processes. These included KEGG OLFACTORY TRANSDUCTION, REACTOME OLFACTORY SIGNALING PATHWAY, NABA SECRETED FACTORS, KEGG CYTOKINE CYTOKINE RECEPTOR INTERACTION and KEGG SYSTEMIC LUPUS ERYTHEMATOSUS (*Figure 4C*). Next, the correlation between the top 10 upregulated and downregulated DEGs and *KLRB1* was examined, revealing significant associations between the majority of DEGs and *KLRB1* (*Figure 4D-4E*).

Link between KLRB1 expression and immune cell infiltration

Additionally, an assessment was conducted to determine if a link existed between *KLRB1* expression levels and the infiltration status of immune cells. We used ssGSEA from the R package and R from Spearman to study the potential association between *KLRB1* expression levels and 24 immune cell types. The findings indicated a substantial link between *KLRB1* expression and all immune cells (*Figure 5A*). Furthermore, heatmap visualization aided in evaluating and illustrating the varying degrees of correlation among the ratios of 24 distinct tumor-infiltrating immune cell subsets (*Figure 5B*).

Nomogram development and validation utilizing the independent factors

A nomogram was developed utilizing independent OS-related factors to enable the prognosis prediction of individuals with BRCA. This predictive tool assigns a higher total score to patients with a less favorable prognosis (*Figure 6A*). To evaluate the prognosis-predictive capacity of the nomogram, calibration curves were employed (*Figure 6B*), confirming its effectiveness in prognosis prediction.

High expression of KLRB1 in BRCA

For assessing the potential utility of *KLRB1* as a biological marker for BRCA, the expression of *KLRB1* in BRCA tissues was further verified using qPCR and IHC. Both qPCR and immunohistochemical outcomes indicated diminished *KLRB1* expression in BRCA (*Figure 7A*,*7B*). Subsequently,

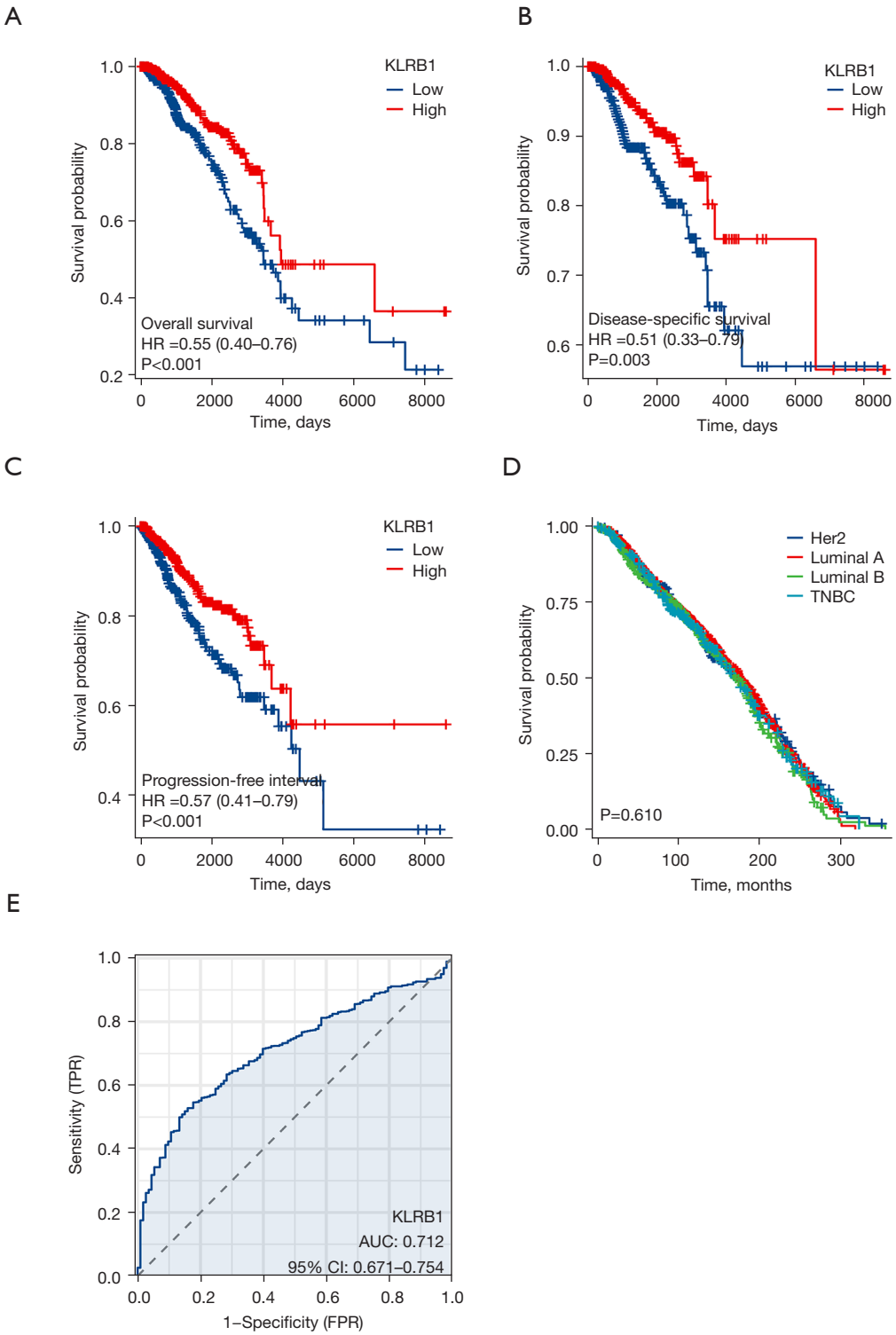

Figure 2 The survival rate of individuals with BRCA with elevated and reduced expression levels of *KLRB1*. (A) OS. (B) DSS. (C) PFI. (D) No significant difference in the prognosis of different breast cancer subtypes in breast cancer patients with low KLRB1 expression. (E) ROC analysis showed that *KLRB1* could accurately distinguish BRCA tumor tissues from healthy tissues. HR, hazard ratio; OS, overall survival; PFI, progression-free interval; DSS, disease-specific survival; BRCA, breast cancer; ROC, receiver operating characteristic.

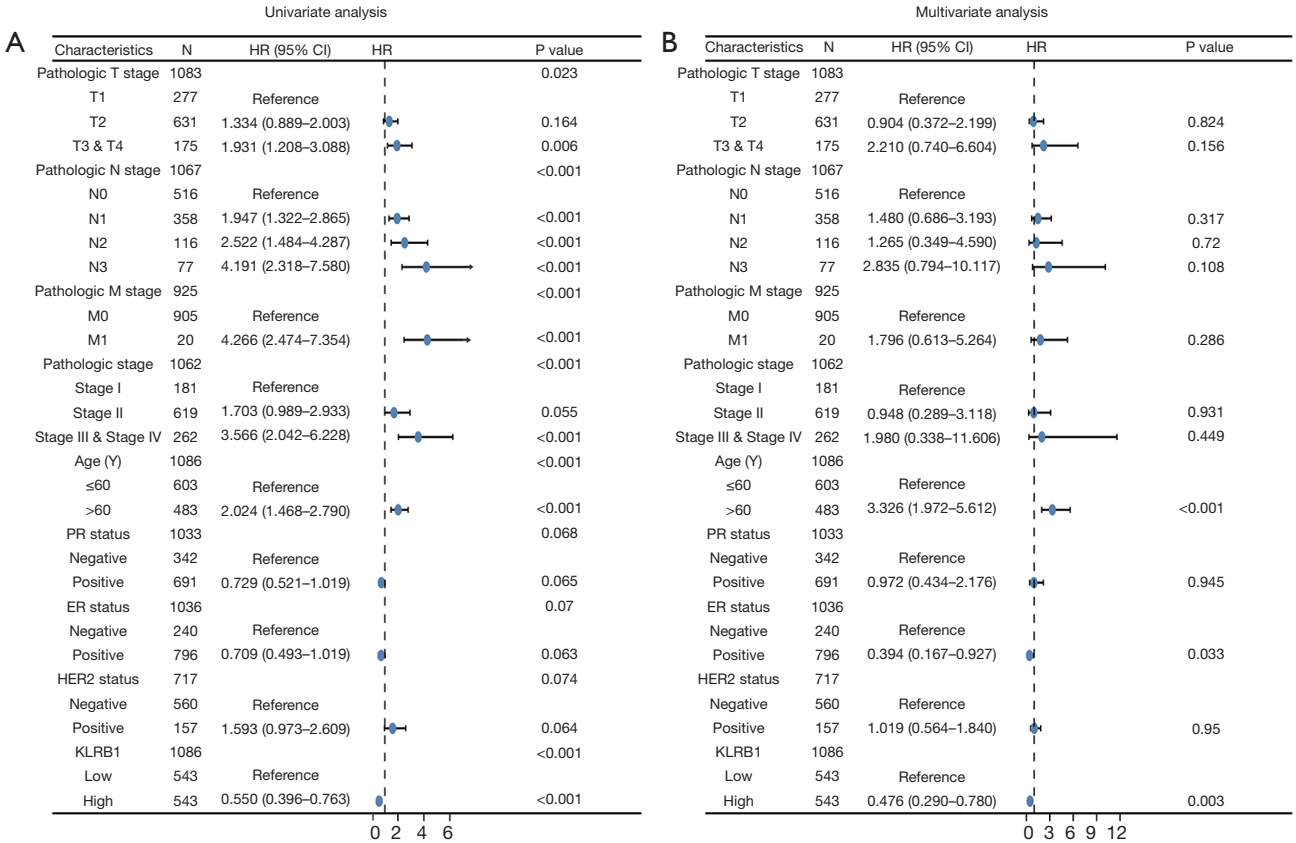

Figure 3 Univariate and multivariate survival analysis. (A) Univariate analysis of OS of individuals with BRCA. (B) Multivariate analysis of OS of individuals with BRCA (P value: log-rank test). HR, hazard ratio; CI, confidence interval; PR, progesterone receptor; ER, estrogen receptor; OS, overall survival; BRCA, breast cancer.

the MCF7 cell line was transfected with a *KLRB1-targeted pEZ-M03 vector*. CCK8 assay showed that the proliferation of MCF7 cells decreased after transfection with KLRB1 (*Figure 7C*). Next, we evaluated the expression of *KLRB1* in MCF10A cell line, MCF7 cell line and MDAMB231 cell line, and found that the expression of *KLRB1* in MCF7 cell line and MDAMB231 cell line was significantly lower than that in MCF10A cell line (*Figure 8A*). qPCR detection of MCF7 cell lines and MDAMB231 cell lines transfected with *KLRB1* targeted pez-m03 vector showed that the expression of *KLRB1* in the cell lines transfected with *KLRB1* was significantly higher than that in the cell lines transfected with vector (*Figure 8B,8C*). CCK8 assay and colony formation assay showed that the proliferation of MDAMB231 cell line decreased after transfection of *KLRB1* (*Figure 8D,8E*). Transwell assay showed that the migration and invasion ability of MDAMB231 cell line decreased after transfected with *KLRB1* (*Figure 8F*).

Discussion

BRCA poses a significant threat to the health of women, being the most prevalent cancer and the second major contributor to cancer-related mortality among females (15,16,17). Therefore, there is a pressing need to identify precise biological markers that can facilitate early detection and continuous monitoring of disease progression. As previous research has indicated, the EMC (ER membrane protein complex subunit) is critically involved in the onset and progression of human cancer (18,19). Limited research has explored the link between the expression of *KLRB1* and the prognosis of BRCA. This study delved into the potential mechanism governing the role of *KLRB1* in promoting BRCA, as well as its feasibility as a potential molecular biological marker.

The comprehensive pan-cancer analysis revealed the consistent downregulation of *KLRB1* across various cancer

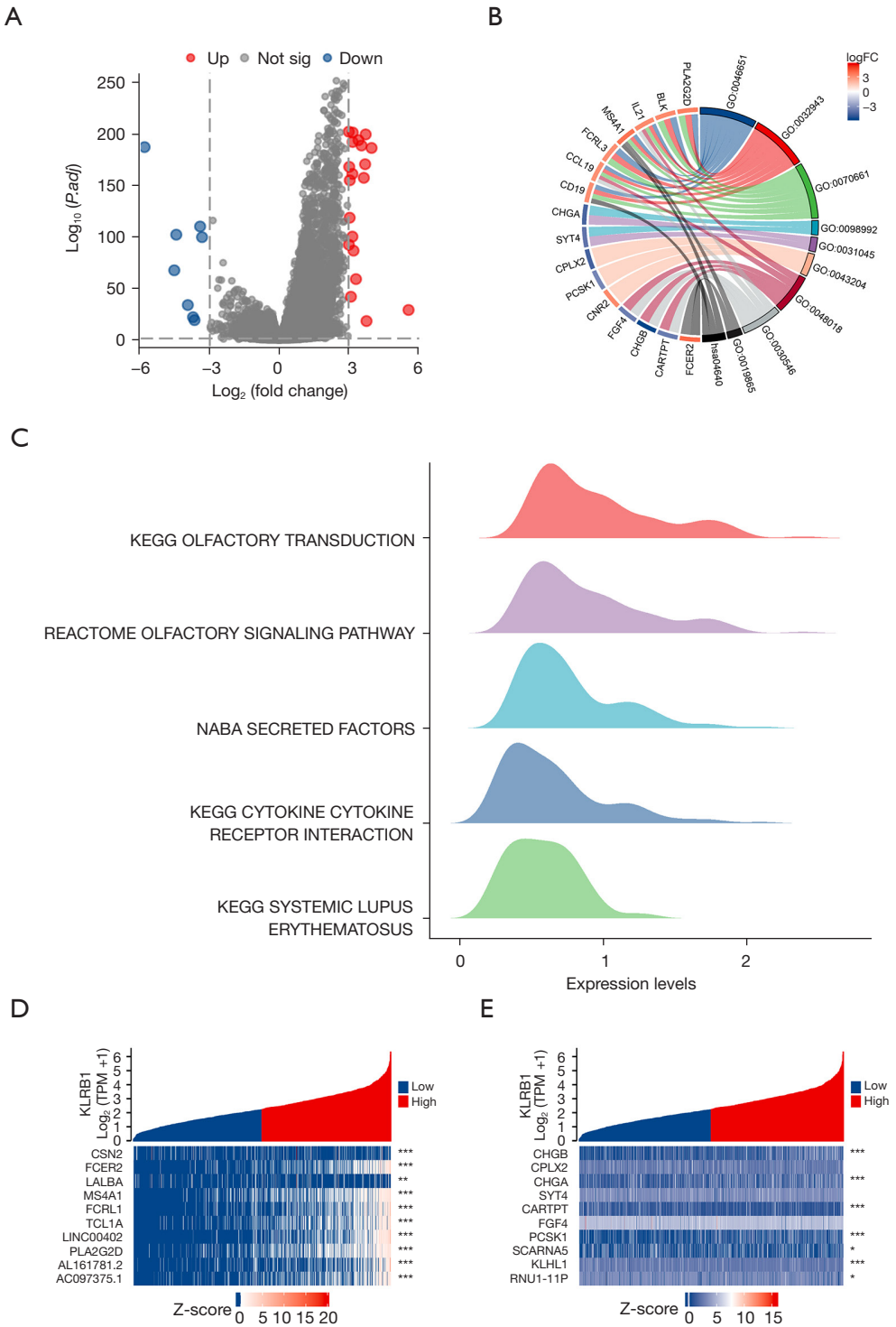

Figure 4 Functional enrichment analysis of *KLRB1*-related DEGs and *KLRB1* in BRCA. (A) Volcano plot. Blue dots and red dots denote DEGs with remarkably reduced and enhanced expression, respectively. (B) GO and KEGG joint analysis. (C) GSEA analysis. (D) Heatmap of the relationship between *KLRB1* expression and the top 10 upregulated DEGs. (E) Heatmap of the association between *KLRB1* expression and the top 10 downregulated DEGs. *, P<0.05; **, P<0.01; ***, P<0.001. DEGs, differentially expressed genes; GO, Gene Ontology; KEGG, Kyoto Encyclopedia of Genes and Genomes; GSEA, gene set enrichment analysis.

Table 3 The results of GO and KEGG joint analysis of DEGs

Ontology	ID	Description	Gene ratio	Bg ratio	P value	P.adjust	Z score
BP	GO:0046651	Lymphocyte proliferation	7/23	296/18,800	4.41e−08	1.91e−05	2.6457513
BP	GO:0032943	Mononuclear cell proliferation	7/23	300/18,800	4.84e−08	1.91e−05	2.6457513
BP	GO:0070661	Leukocyte proliferation	7/23	330/18,800	9.28e−08	2.36e−05	2.6457513
CC	GO:0098992	Neuronal dense core vesicle	2/23	13/19,594	0.0001	0.0049	−1.4142136
CC	GO:0031045	Dense core granule	2/23	26/19,594	0.0004	0.0101	−1.4142136
CC	GO:0043204	Perikaryon	3/23	153/19,594	0.0007	0.0118	−0.5773503
MF	GO:0048018	Receptor ligand activity	5/20	489/18,410	0.0001	0.0051	−0.4472136
MF	GO:0030546	Signaling receptor activator activity	5/20	496/18,410	0.0002	0.0051	−0.4472136
MF	GO:0019865	Immunoglobulin binding	2/20	24/18,410	0.0003	0.0067	1.4142136
KEGG	hsa04640	Hematopoietic cell lineage	3/12	99/8,164	0.0004	0.0116	1.7320508

GO, Gene Ontology; KEGG, Kyoto Encyclopedia of Genes and Genomes; DEG, differentially expressed gene; BP, biological process; CC, cellular component; MF, molecular function.

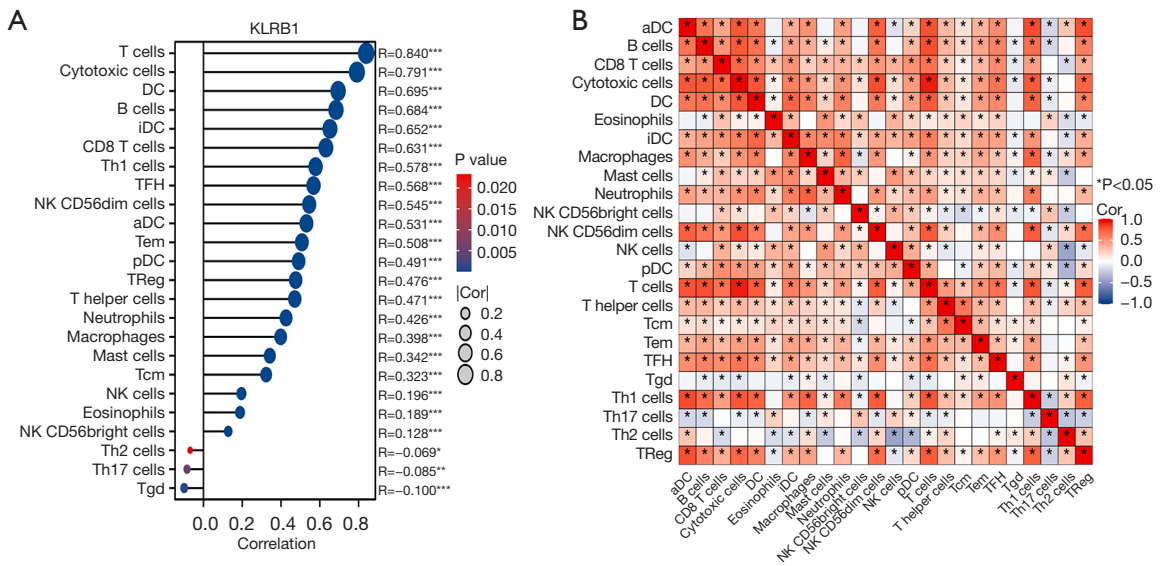

Figure 5 *KLRB1* expression was associated with immune cell infiltration. (A) Lollipop chart of *KLRB1* expression levels in 24 immune cell types. (B) Heatmap of 24 infiltrating immune cells in BRCA and *KLRB1* have the pivotal function in the immune infiltration in BRCA. *, P<0.05; **, P<0.01; ***, P<0.001. BRCA, breast cancer.

types. Notably, elevated *KLRB1* expression correlated with improved OS in individuals with BRCA. Analysis of various clinical stages revealed a substantial correlation between *KLRB1* expression and clinical stages. Univariate and multivariate Cox analyses affirmed the independent prognosis-predictive value of *KLRB1* in predicting the prognosis of individuals. Collectively, these findings, along with the ROC analysis outcomes, strongly imply that *KLRB1* holds promise as a potential prognostic biological marker for individuals with BRCA.

This study revealed a significant inhibitory effect of the *KLRB1* gene on cell proliferation in BRCA cells. Simultaneously, this research aims to ascertain the association between the expression of the *KLRB1* gene and the clinical prognosis of individuals with BRCA, indicating that individuals with higher *KLRB1* expression experience

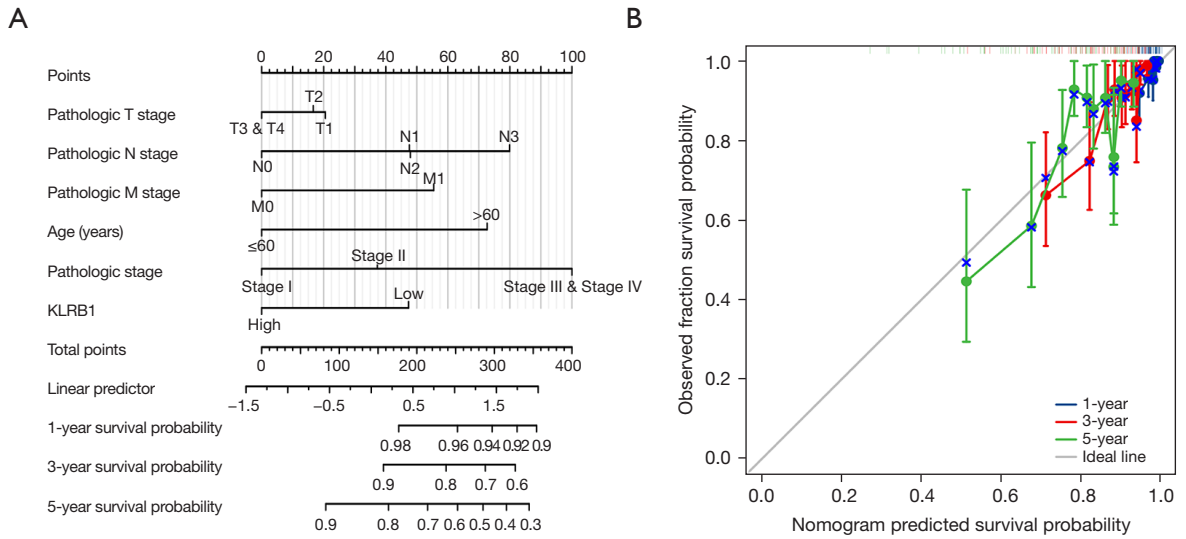

Figure 6 A nomogram and calibration curves for the prediction of one-, three-, and five-year OS rates of individuals with BRCA. (A) A nomogram for the prediction of the one-, three-, and five-year OS rates of individuals with BRCA. (B) Calibration curves of the nomogram prediction of one-, three-, and five-year OS rates of individuals with BRCA. OS, overall survival; BRCA, breast cancer.

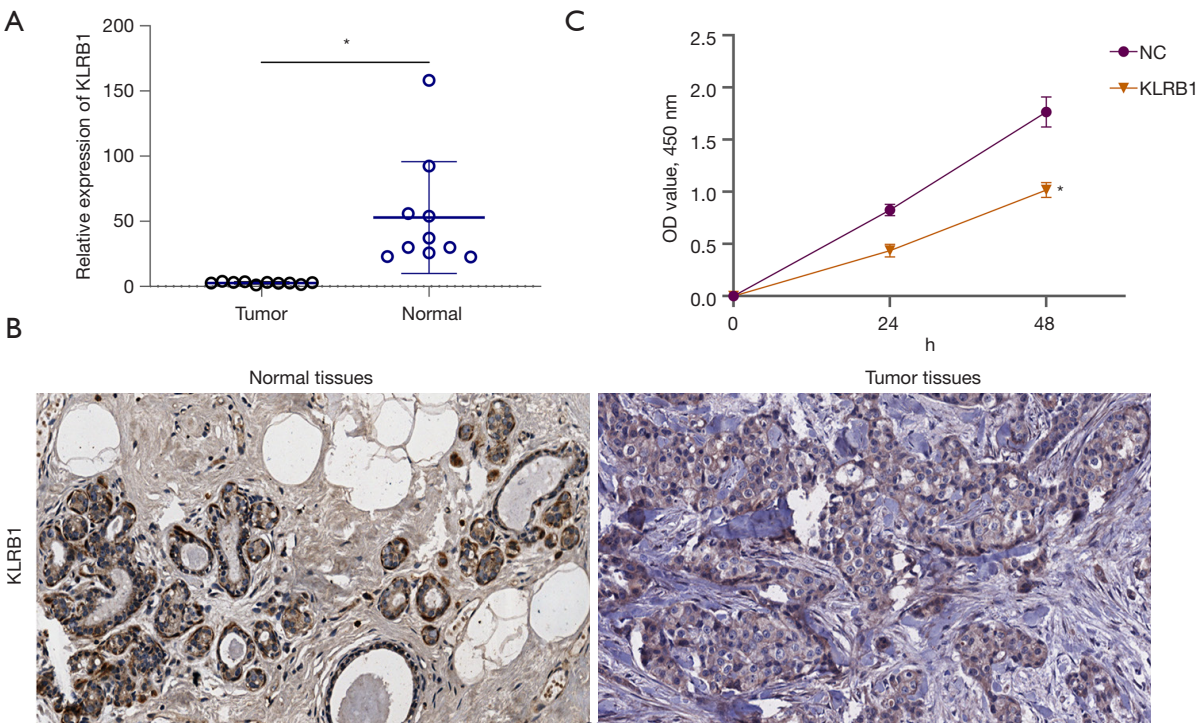

Figure 7 BRCA exhibits lowered expression levels of *KLRB1*. (A) The expression of *KLRB1* mRNA was assessed by qPCR. (B) The expression of *KLRB1* proteins was assessed by IHC. (Magnification: ×40). (C) Decreased proliferation of MCF7 cells transfected with *KLRB1* vector. *P<0.05. BRCA, breast cancer; mRNA, messenger RNA; qPCR, quantitative polymerase chain reaction; IHC, immunohistochemistry.

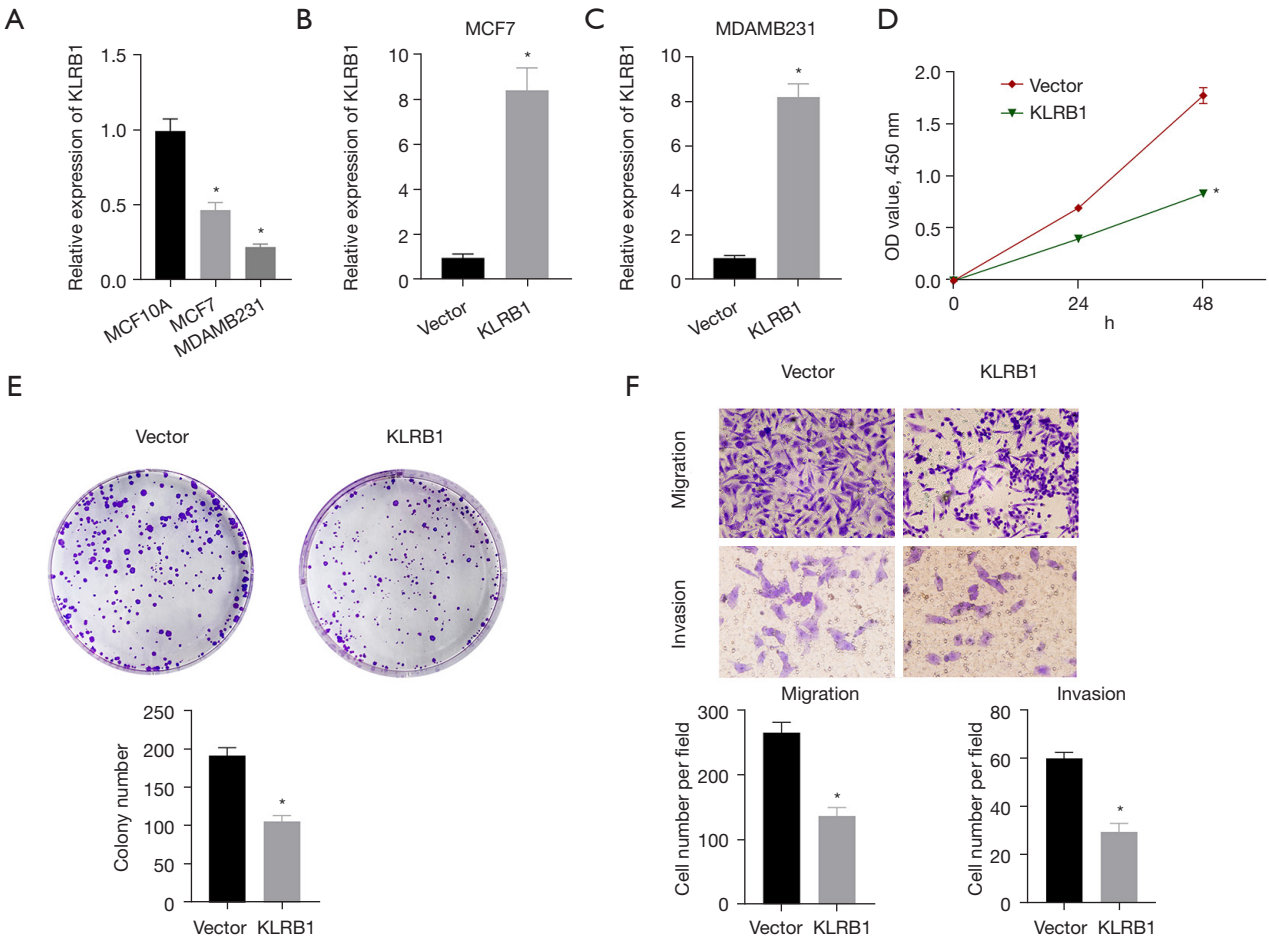

Figure 8 Overexpression of *KLRB1* inhibits the progression of breast cancer cells. (A) The expression of *KLRB1* in MCF10A cells, MCF7 cells and MDAMB231 cells. (B,C) The expression level of *KLRB1* after transfection in MCF7 cells and MCF10A cells. (D,E) Decreased proliferation of MDAMB231 cells transfected with *KLRB1* vector (0.1% crystal violet staining). (F) *KLRB1* inhibits the migration and invasion ability of both MCF7 and MDAMB231 cells (0.1% crystal violet staining, ×10). *, P<0.05.

a more favorable prognosis. These findings will serve as a crucial foundation for further investigating the mechanism of the *KLRB1* gene in BRCA and identifying potential therapeutic targets.

The results of GSEA suggested that *KLRB1*-related differential genes were involved in KEGG organic transformation, Reactome organic signaling pathway, NABA restricted factors, KEGG cytokine-cytokine receptor interaction, and KEGG systemic lupus erythematosus pathways. These pathways widely impact cell proliferation, migration, differentiation, and metabolism. In BRCA, olfactory transduction mediated signal transduction ultimately leads to olfactory perception by recognizing odor molecules and activating signal transduction pathways, which also regulates the apoptotic cycle of olfactory sensory neurons in an olfactory receptor-specific manner. A recent study has indicated that certain olfactory receptors exhibit expression in tissues other than the olfactory epithelium, implying their potential for pleiotropic effects (20). In addition, the cytokine-cytokine receptor interaction signaling pathway is also related to BRCA treatment. Various methods can enhance the growth inhibitory and immunostimulatory effects of interferon and interleukin or inhibit the inflammatory and tumor effects of cytokines, thereby treating BRCA (21,22).

Furthermore, the link between *KLRB1* expression and the level of immune infiltration in BRCA was investigated utilizing two approaches, ssGSEA and Spearman. *KLRB1*

exhibited the highest positive correlation with T cells and cytotoxic cells. T cells are a major subclass of lymphocytes, possessing diverse biological functions, including directly targeting and killing specific cells, aiding or inhibiting antibody production by B cells, responding to specific antigens and mitogens, and generating cytokines (23). Research has demonstrated that T cells can directly inhibit BRCA cells and improve the prognosis of BRCA individuals (24,25). Cytotoxic T lymphocyte (CTL) is a specific T cell that secretes various cytokines to participate in immunity and has a strong anti-tumor effect (26). Study has shown that CTL can effectively inhibit BRCA cells and inhibit the onset and angiogenesis of BRCA (27).

Finally, the results were validated by qPCR, IHC, and CCK8 assays. The study demonstrated a significant decrease in *KLRB1* expression in corresponding non-tumor tissues. Additionally, the enhanced expression of *KLRB1* led to a decrease in the proliferation and invasion capacity of BRCA MCF7 cells. These collective findings highlight that *KLRB1* holds promise as a potential predictive tumor marker for individuals with BRCA.

In conclusion, the study aimed to investigate the mechanism and potential therapeutic targets associated with the *KLRB1* gene in BRCA. Through the examination of *KLRB1* gene expression and function, the aim is to unveil its crucial involvement in the onset and development of BRCA. This endeavor also aspires to offer novel approaches and techniques for addressing the treatment of BRCA. Nonetheless, the precise mechanism via which *KLRB1* influences the tumor immune microenvironment and the progression of tumors in BRCA remains to be fully understood. Additional fundamental research and clinical trials are warranted to comprehensively unravel the biological impacts of *KLRB1* in BRCA.

Conclusions

In summary, the elevated expression level of *KLRB1* is related to prognostic significance and *KLRB1* is positively linked to T cells and cytotoxic cells. Consequently, *KLRB1*, potentially linked to immune infiltration, could serve as a predictive indicator for individuals with BRCA.

Acknowledgments

Funding: This work was supported by the Natural Science Foundation of Liaoning Province (No. 2019-ZD-1020).

Footnote

Reporting Checklist: The authors have completed the TRIPOD reporting checklist. Available at https://tcr.amegroups.com/article/view/10.21037/tcr-23-1231/rc

Data Sharing Statement: Available at https://tcr.amegroups.com/article/view/10.21037/tcr-23-1231/dss

Peer Review File: Available at https://tcr.amegroups.com/article/view/10.21037/tcr-23-1231/prf

Conflicts of Interest: All authors have completed the ICMJE uniform disclosure form (available at https://tcr.amegroups.com/article/view/10.21037/tcr-23-1231/coif). The authors report funding from the Natural Science Foundation of Liaoning province (No. 2019-ZD-1020). The authors have no other conflicts of interest to declare.

Ethical Statement: The authors are accountable for all aspects of the work in ensuring that questions related to the accuracy or integrity of any part of the work are appropriately investigated and resolved. The study was conducted in accordance with the Declaration of Helsinki (as revised in 2013). The approval for this research was granted by the ethics committee of Liaoning Cancer Hospital (20210621) and written informed consent was obtained from every participant.

References

1. Siegel RL, Miller KD, Fuchs HE, et al. Cancer Statistics, 2021. CA Cancer J Clin 2021;71:7-33.
2. Cao W, Chen HD, Yu YW, et al. Changing profiles of cancer burden worldwide and in China: a secondary analysis of the global cancer statistics 2020. Chin Med J (Engl) 2021;134:783-91.

3. Loibl S, Poortmans P, Morrow M, et al. Breast cancer. Lancet 2021;397:1750-69.
4. Coughlin SS. Epidemiology of Breast Cancer in Women. Adv Exp Med Biol 2019;1152:9-29.
5. Mathewson ND, Ashenberg O, Tirosh I, et al. Inhibitory CD161 receptor identified in glioma-infiltrating T cells by single-cell analysis. Cell 2021;184:1281-1298.e26.
6. Di W, Fan W, Wu F, et al. Clinical characterization and immunosuppressive regulation of CD161 (KLRB1) in glioma through 916 samples. Cancer Sci 2022;113:756-69.
7. Zhou X, Du J, Liu C, et al. A Pan-Cancer Analysis of CD161, a Potential New Immune Checkpoint. Front Immunol 2021;12:688215.
8. Zhao H, Yin X, Wang L, et al. Identifying tumour microenvironment-related signature that correlates with prognosis and immunotherapy response in breast cancer. Sci Data 2023;10:119.
9. Junjun S, Yangyanqiu W, Jing Z, et al. Prognostic model based on six PD-1 expression and immune infiltration-associated genes predicts survival in breast cancer. Breast Cancer 2022;29:666-76.
10. Li W, Guo X, Chen C, et al. The prognostic value of arachidonic acid metabolism in breast cancer by integrated bioinformatics. Lipids Health Dis 2022;21:103.
11. Gentles AJ, Newman AM, Liu CL, et al. The prognostic landscape of genes and infiltrating immune cells across human cancers. Nat Med 2015;21:938-45.
12. Li Y, Gao Y, Niu X, et al. LncRNA BASP1-AS1 interacts with YBX1 to regulate Notch transcription and drives the malignancy of melanoma. Cancer Sci 2021;112:4526-42.
13. Li YL, Gao YL, Niu XL, et al. Identification of Subtype-Specific Metastasis-Related Genetic Signatures in Sarcoma. Front Oncol 2020;10:544956.
14. Yang Y, Li Y, Qi R, et al. Development and Validation of a Combined Glycolysis and Immune Prognostic Model for Melanoma. Front Immunol 2021;12:711145.
15. Krastev T, van Turnhout A, Vriens E, et al. Long-term Follow-up of Autologous Fat Transfer vs Conventional Breast Reconstruction and Association With Cancer Relapse in Patients With Breast Cancer. JAMA Surg 2019;154:56-63.
16. Fahad Ullah M. Breast Cancer: Current Perspectives on the Disease Status. Adv Exp Med Biol 2019;1152:51-64.
17. Britt KL, Cuzick J, Phillips KA. Key steps for effective breast cancer prevention. Nat Rev Cancer 2020;20:417-36.
18. Wang X, Xia Y, Xu C, et al. ER membrane protein complex subunit 6 (EMC6) is a novel tumor suppressor in gastric cancer. BMB Rep 2017;50:411-6.
19. Shen MX, Ding JB. Expression levels and roles of EMC-6, Beclin1, and Rab5a in the cervical cancer. Eur Rev Med Pharmacol Sci 2017;21:3038-46.
20. Ranzani M, Iyer V, Ibarra-Soria X, et al. Revisiting olfactory receptors as putative drivers of cancer. Wellcome Open Res 2017;2:9.
21. Propper DJ, Balkwill FR. Harnessing cytokines and chemokines for cancer therapy. Nat Rev Clin Oncol 2022;19:237-53.
22. Conlon KC, Miljkovic MD, Waldmann TA. Cytokines in the Treatment of Cancer. J Interferon Cytokine Res 2019;39:6-21.
23. Chapman NM, Boothby MR, Chi H. Metabolic coordination of T cell quiescence and activation. Nat Rev Immunol 2020;20:55-70.
24. Tchou J, Zhao Y, Levine BL, et al. Safety and Efficacy of Intratumoral Injections of Chimeric Antigen Receptor (CAR) T Cells in Metastatic Breast Cancer. Cancer Immunol Res 2017;5:1152-61.
25. Sconocchia G, Lanzilli G, Cesarini V, et al. Direct CD32 T-cell cytotoxicity: implications for breast cancer prognosis and treatment. Life Sci Alliance 2022;5:e202201590.
26. Reina-Campos M, Scharping NE, Goldrath AW. CD8(+) T cell metabolism in infection and cancer. Nat Rev Immunol 2021;21:718-38.
27. Palazon A, Tyrakis PA, Macias D, et al. An HIF-1α/VEGF-A Axis in Cytotoxic T Cells Regulates Tumor Progression. Cancer Cell 2017;32:669-683.e5.

Cite this article as: Liu X, Cui Q, Qin N. Low expression of *KLRB1* predicts poor survival outcomes and is associated with immune infiltration in breast cancer. Transl Cancer Res 2024;13(3):1225-1240. doi: 10.21037/tcr-23-1231

